AIAA Guidance, Navigation and Control Conference and Exhibit
20 - 23 August 2007, Hilton Head, South Carolina

AIAA 2007-6646

Optimization of the Time-Delay Margin of $\mathcal{L}_1$ Adaptive Controller via the Design of the Underlying Filter*

Dapeng Li, Vijay V. Patel, Chengyu Cao, Naira Hovakimyan
Dept. of Aerospace and Ocean Engineering, Virginia Tech, Blacksburg, VA 24061, USA
Kevin Wise
Integrated Defense Systems, The Boeing Company

Recent papers[1–4] have introduced a new paradigm for design of adaptive controllers that enables *a priori* prediction of performance bounds and also analytical quantification of the time-delay margin of the closed-loop nonlinear system. In this paper, we revisit the main architecture from Refs.[1,2] and consider several filter design methods for maximizing the time-delay margin, while retaining the same performance bounds.

I. Introduction

Direct Model Reference Adaptive Control (MRAC) schemes have proven to be extremely useful in a number of flight tests for recovering nominal performance in the presence of modeling and environmental uncertainties (see Ref.[5,6] and references therein). A major challenge in analysis of these systems is determining their stability margins, which is directly dependent upon the adaptive control learning rate. Today this analysis largely relies on the numerical sensitivity provided by Monte-Carlo analysis. The MRAC adaptive gain algorithm typically has the following form

$$\dot{\hat{k}}_x(t) = -\Gamma e^\top(t) P b x(t), \tag{1}$$

where Γ is the adaptive learning rate, x is the state vector, $e(t) = x(t) - x_{ref}(t)$ is the tracking error, $x_{ref}(t)$ is the state of the reference model, P is the solution of the algebraic Lyapunov equation, and b the control distribution matrix. One would naturally like to use a large learning rate in order to drive the error $e(t) = x(t) - x_{ref}(t)$ to zero as quickly as possible, forcing the state $x(t)$ to track the state $x_{ref}(t)$ of the reference model.

In the recent application of MRAC to the JDAM munition, Ref.,[6] the MRAC algorithms with large learning rates were found to be sensitive to time-delay. This was discovered during hardware-in-the-loop bench simulations, in which a larger than normal time delay is present due to the laboratory setup. It was later reproduced in 6DOF simulation analysis focused on determining the time-delay margins. The MRAC learning rates were then "tuned" using the 6DOF to reduce the sensitivity and provide adequate margin. It has also been observed in practice that large learning rates can produce high-frequency oscillations in the control signal. In systems that use electric actuation this high frequency oscillation significantly increases the current draw and is undesirable.

Thus, a major challenge in analysis of these systems is determining the stability margins, gain and time-delay, which are known to depend upon the adaptive control learning rate Γ. Refs.[1,2] addressed this challenge and introduced a new paradigm for design of adaptive controllers, the resulting architecture being named $\mathcal{L}_1$ adaptive control. The $\mathcal{L}_1$ adaptive control architectures adapt fast, leading to desired transient performance with analytically computable performance bounds. Moreover, as demonstrated in Ref.,[3,4] unlike the standard MRAC algorithms, the $\mathcal{L}_1$ adaptive control architectures have guaranteed time-delay margin in the presence of fast adaptation. The $\mathcal{L}_1$ adaptive controller and its variants have been used for control of wing rock,[7] aerial refueling,[8] and also flight tested on a miniature unmanned air vehicle.[9]

In this paper, we develop a design technique for the underlying filter in the $\mathcal{L}_1$ adaptive control architecture that maximizes the time-delay margin, while retaining the same performance bounds. We consider several filters, and using

*This material is based upon work supported by the United States Air Force under Contracts No. FA9550-05-1-0157 and ONR under Contract N00014-05-1-0828. Any opinions, findings and conclusions or recommendations expressed in this material are those of the authors and do not necessarily reflect the views of the United States Air Force and ONR. Corresponding author e-mail: dpli@vt.edu.

frequency domain tools along with nonlinear optimization methods, we compare the performance of the different filters towards obtaining the largest time-delay margin.

The rest of the paper is organized as follows. In Section II, we introduce the $\mathcal{L}_1$ adaptive control architecture from Refs.[1–4] and its associated time-delay margin. In Section III, we introduce the problem formulation addressed in this paper. In section IV, we give an overview of multi-objective optimization used to optimize the filter coefficients. In Section V, we present an optimization method for filter design. Then a filter design procedure based on multi-objective optimization is given in Section VI, where filters with different forms and design methods are compared and evaluated. Conclusions are summarized in Section VII.

II. $\mathcal{L}_1$ Adaptive Control Architecture, Its Performance Bounds and Time-delay Margin

Consider the following single-input single-output system dynamics:

$$\begin{aligned} \dot{x}(t) &= A_m x(t) - b\theta^\top x(t) + bu(t), \quad x(0) = x_0 \\ y(t) &= c^\top x(t)\,, \end{aligned} \tag{2}$$

where $x \in \mathbb{R}^n$ is the system state vector (measurable), $u \in \mathbb{R}$ is the control signal, $b, c \in \mathbb{R}^n$ are known constant vectors, A_m is a given $n \times n$ Hurwitz matrix, $y \in \mathbb{R}$ is the regulated output, and the unknown parameter θ belongs to a given compact convex set $\theta \in \Theta$. Let

$$\begin{aligned} \dot{x}_m(t) &= A_m x_m(t) + bk_g r(t), \quad x_m(0) = x_0\,, \\ y_m(t) &= c^\top x_m(t) \end{aligned} \tag{3}$$

be the desired reference system, where $x_m \in \mathbb{R}^n$, A_m is the same as in (2), k_g is a design gain

$$k_g = \lim_{s\to 0} \frac{1}{c^\top H(s)} = \frac{1}{c^\top H(0)}\,, \tag{4}$$

and

$$H(s) = (s\mathbb{I} - A_m)^{-1} b\,. \tag{5}$$

For the linearly parameterized system in (2), we consider the following state predictor

$$\begin{aligned} \dot{\hat{x}}(t) &= A_m \hat{x}(t) + b(u(t) - \hat{\theta}^\top(t) x(t))\,, \quad \hat{x}(0) = x_0 \\ \hat{y}(t) &= c^\top \hat{x}(t)\,, \end{aligned} \tag{6}$$

in which the adaptive law for $\hat{\theta}(t)$ is given by

$$\dot{\hat{\theta}}(t) = \Gamma \mathrm{Proj}(\hat{\theta}(t), x(t)\tilde{x}^\top(t) Pb), \quad \hat{\theta}(0) = \hat{\theta}_0\,, \tag{7}$$

where $\tilde{x}(t) = \hat{x}(t) - x(t)$ is the prediction error, $\Gamma \in \mathbb{R}^{n\times n} = \Gamma_c I_{n\times n}$ is the matrix of adaptation gains, $P = P^\top$ is the solution of the algebraic equation $A_m^\top P + PA_m = -Q$, $Q > 0$, while projection denotes the projection operator.[10] Letting

$$\bar{r}(t) = \hat{\theta}^\top(t) x(t), \tag{8}$$

we consider the following filtered adaptive controller:

$$u(s) = C(s)\big(\bar{r}(s) + k_g r(s)\big)\,, \tag{9}$$

where $u(s)$, $\bar{r}(s), r(s)$ are the Laplace transformations of $u(t)$, $\bar{r}(t), r(t)$, respectively, $C(s)$ is a stable and strictly proper system with low-pass gain $C(0) = 1$, and k_g is the same as in (4). Letting

$$\theta_{\max} = \max_{\theta\in\Omega} \sum_{i=1}^{n} |\theta_i|\,,$$

where θ_i is the i^{th} element of θ, the complete $\mathcal{L}_1$ adaptive controller consists of (6), (7), (9) subject to the following $\mathcal{L}_1$-gain stability criterion:

$$\lambda = \|H(s)(1 - C(s))\|_{\mathcal{L}_1} \theta_{\max} < 1\,, \tag{10}$$

where $\|H(s)(1-C(s))\|_{\mathcal{L}_1}$ is the $\mathcal{L}_1$ gain of the stable transfer function $H(s)(1-C(s))$, which restricts the choice of the filter $C(s)$.[1,2]

We define a linear time-invariant reference system using the non-adaptive version of (9)

$$x_{ref}(s) = H(s)\left(k_g C(s) r(s) + (C(s)-1)\theta^\top x_{ref}(s)\right) \quad (11)$$
$$u_{ref}(s) = C(s)\left(k_g r(s) + \theta^\top x_{ref}(s)\right) \quad (12)$$

along with the desired system

$$y_{des}(s) = c^\top G(s) r(s) = C(s) k_g c^\top H_o(s) r(s)\,, \quad (13)$$
$$u_{des}(s) = k_g C(s)\left(1 + C(s)\theta^\top H_o(s) - K^\top H_o(s)\right) r(s). \quad (14)$$

The main result from Refs.[1,2] claims that subject to (10) one has

$$\lim_{\Gamma_c\to\infty}(x(t) - x_{ref}(t)) = 0\,, \quad \forall\, t \geq 0\,,$$
$$\lim_{\Gamma_c\to\infty}(u(t) - u_{ref}(t)) = 0\,, \quad \forall\, t \geq 0\,,$$

along with the following performance bounds

$$\|y_{ref} - y_{des}\|_{\mathcal{L}_\infty} \leq \frac{\lambda}{1-\lambda}\|c^\top\|_{\mathcal{L}_1}\|G(s)\|_{\mathcal{L}_1}\|r\|_{\mathcal{L}_\infty}\,, \quad (15)$$
$$\|y_{ref} - y_{des}\|_{\mathcal{L}_\infty} \leq \frac{1}{1-\lambda}\|c^\top\|_{\mathcal{L}_1}\|h_3\|_{\mathcal{L}_\infty}\,, \quad (16)$$
$$\|u_{ref} - u_{des}\|_{\mathcal{L}_\infty} \leq \frac{\lambda}{1-\lambda}\|C(s)\theta^\top - K^\top\|_{\mathcal{L}_1}\|G(s)\|_{\mathcal{L}_1}\|r\|_{\mathcal{L}_\infty}\,, \quad (17)$$
$$\|u_{ref} - u_{des}\|_{\mathcal{L}_\infty} \leq \frac{1}{1-\lambda}\|C(s)\theta^\top - K^\top\|_{\mathcal{L}_1}\|h_3\|_{\mathcal{L}_\infty}\,, \quad (18)$$

where $h_3(t)$ is the inverse Laplace transformation of

$$H_3(s) = (C(s)-1)C(s)r(s)k_g H_o(s)\theta^\top H_o(s). \quad (19)$$

We notice that when $C(s) = 1$, $u_{ref}(t)$ reduces to the following *ideal* controller

$$u_{ideal}(t) = k_g r(t) + \theta^\top x_{ref}(t)\,, \quad (20)$$

and (11) reduces to (3) by cancelling the uncertainties exactly. We note that the control law $u_{ref}(t)$ is not implementable since its definition involves the unknown parameters. However, the $\mathcal{L}_1$ adaptive controller ensures that $x(t)$ and $u(t)$ track the state $x_{ref}(t)$ and the control signal $u_{ref}(t)$ of this reference system both in transient and steady-state, if the adaptation rate is selected sufficiently large. Reference[2] further provides design guidelines for selection of $C(s)$ to ensure that the output of the reference system in (11) can satisfy desired control specifications. The $\mathcal{L}_1$ adaptive control architecture is illustrated in Fig. 1, and its complete design and analysis framework is developed in Refs.[1,2]

Thus, for performance improvement one needs to minimize λ, which can be conservatively upper bounded

$$\lambda = \|(H(s)(1-C(s))\|_{\mathcal{L}_1}\theta_{\max} = \|H(s)(C(s)-1)\|_{\mathcal{L}_1}\theta_{\max} \leq \|H(s)\|_{\mathcal{L}_1}\|C(s)-1\|_{\mathcal{L}_1}\theta_{\max}. \quad (21)$$

Minimization of λ can be achieved from two different perspectives: i) fix $C(s)$ and minimize $\|H(s)\|_{\mathcal{L}_1}$, ii) fix $H(s)$ and minimize the $\mathcal{L}_1$-gain of one of the cascaded systems $\|H(s)(C(s)-1)\|_{\mathcal{L}_1}$, $\|(C(s)-1)r(s)\|_{\mathcal{L}_1}$ or $\|C(s)(C(s)-1)\|_{\mathcal{L}_1}$ via the choice of $C(s)$. We further notice that $C(s) = 1$ achieves the best performance.

The time-delay margin of $\mathcal{L}_1$ adaptive controller is introduced in Ref.[4] and is given by:

$$\mathcal{T}(H_o(s)) = \mathcal{P}(H_o(s))/\omega_c\,, \quad \bar{H}(s) = (s\mathbb{I} - A_m - b\theta^\top)^{-1}b\,, \quad (22)$$

where $\mathcal{P}(H_o(s))$ is the phase margin of the open-loop system

$$H_o(s) = C(s)(1 + \theta^\top \bar{H}(s))/(1 - C(s)),$$

and ω_c is the cross-over frequency of $H_o(s)$. It is obvious that while increasing the bandwidth of $C(s)$ for performance improvement, the time-delay margin will be reduced.

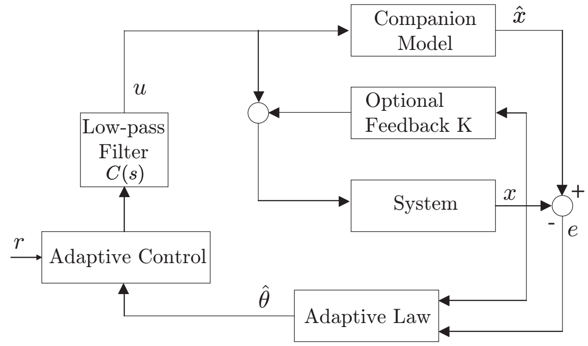

Figure 1. Closed-loop system with $\mathcal{L}_1$ adaptive controller

III. Illustration for a Scalar Example

We now give an illustrative example to show the relation between the bandwidth of the filter $C(s)$, the $\mathcal{L}_1$-gain and the time-delay margin. Consider the following scalar system:

$$\dot{x}(t) = ax(t) + b\theta + u(t). \tag{23}$$

The state predictor is:

$$\dot{\hat{x}}(t) = a_m\hat{x}(t) + (a - a_m)x(t) + b\hat{\theta}(t) + u(t), \tag{24}$$

and let the low-pass filter be

$$C(s) = \frac{w}{s+w}, \quad w > 0. \tag{25}$$

Let $a = 1$, $a_m = -2$, $b = 1$ and $\theta = 0.5$. We have

$$H(s) = \frac{1}{s+2}$$

$$\bar{H}(s) = \frac{1}{s - a_m - b\theta} = \frac{1}{s + 1.5}.$$

Fig. 2 shows the $\mathcal{L}_1$ gain of $\|H(s)(1 - C(s))\|_{\mathcal{L}_1}$ and the time-delay margin of $H_o(s)$ in (22) as the bandwidth of $C(s)$ changes. We observe that the choice of the filter $C(s)$ is crucial both in the performance bounds and in the time-delay margin, as predicted by theory. One needs smaller $\mathcal{L}_1$ gain to accommodate larger uncertainties, and larger time-delay margin for robustness. Considering this trade-off of $\mathcal{L}_1$-gain and time-delay margin, in the next section we introduce a multi-objective optimization method for design of $C(s)$ that retains the same $\mathcal{L}_1$-gain for the performance bounds in (15), (16), (17), (18) and maximizes the time-delay margin in (22).

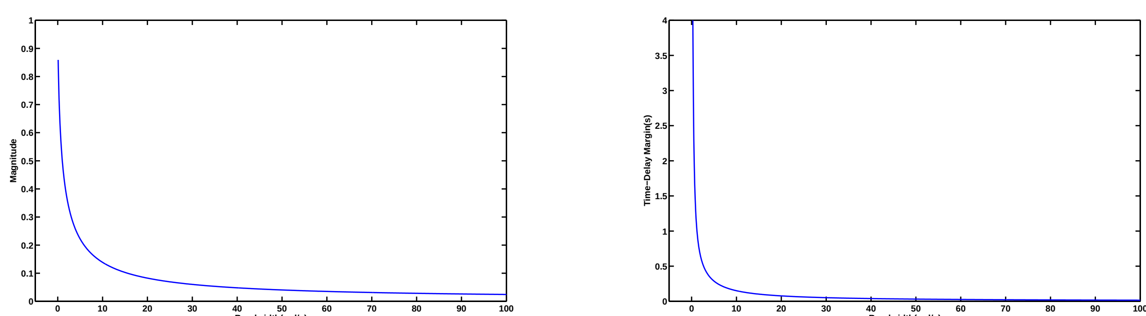

(a) $\|H(s)(1 - C(s))\|_{\mathcal{L}_1}$ (b) Time-delay Margin

Figure 2. $\mathcal{L}_1$ Gain and time-delay margin

IV. Review of Multi-Objective Optimization

In this section, a brief review of multi-objective optimization is given. The general form of the constrained, nonlinear, multiple-objective optimization problem can be stated as follows:

$$\min_x f_i(x) \quad i = 1, 2, ..., p \tag{26}$$

subject to

$$x \in \mathcal{X} = \{x | x \in \mathbb{R}^m, g_j(x) \leq 0, \quad j = 1, 2, ..., m\}. \tag{27}$$

There are p objective functions $f_i, \ i = 1, 2, ..., p$ that must be minimized simultaneously. The minimization takes place over $\mathcal{X} \subset \mathbb{R}^m$, $\mathcal{X}$ reflects the m functional constraints, $g_j(x)$, on the decision variables $x \in \mathcal{X}$.

The most widely-used method for multi-objective optimization is the weighted sum method. The method transforms multiple objectives into an aggregated objective function by multiplying each objective function by a weighting factor and summing up all weighted objective functions:

$$f_w(x) = \sum_{n=1}^{p} \alpha_i f_i(x), \tag{28}$$

where $\alpha_i, \ (i = 1, ..., p)$, is the weighting factor for the i^{th} objective function. If $\sum_{i=1}^{p} \alpha_i = 1$ and $0 \leq \alpha \leq 1$, the weighted sum is said to be a convex combination of objective functions. This method will be explored in this paper later.

V. Filter Structure Design Via $\|C(s)(1 - C(s))\|_{\mathcal{L}_1}$ Minimization

From (15), (16), (17) and (18) it is obvious that one can improve the performance bounds by minimizing the $\mathcal{L}_1$-gain $\|(C(s) - 1)C(s)\|_{\mathcal{L}_1}$. For minimization of $\|C(s)(C(s) - 1)\|_{\mathcal{L}_1}$ notice that if $C(s)$ is an ideal low-pass filter, then $C(s)(C(s) - 1) = 0$ and hence $\|h_3\|_{\mathcal{L}_\infty} = 0$. Since an ideal low-pass filter is not physically implementable, one can minimize $\|C(s)(C(s) - 1)\|_{\mathcal{L}_1}$ via appropriate choice of $C(s)$.

So we consider the $\|C(s)(1 - C(s))\|_{\mathcal{L}_1}$ minimization for different classes of filters. First notice that if $C(s)$ is an ideal low-pass filter, it can be checked easily that $C(s)(1 - C(s)) = 0$. Although an ideal low-pass filter is not physically implementable, one can still minimize $\|C(s)(1 - C(s))\|_{\mathcal{L}_1}$ via the choice of the low-pass filter $C(s)$. We consider the following filters:

1. $$C_1(s) = \frac{\theta_n(0)}{\theta_n(s/\omega_0)} \tag{29}$$

   where $\theta_n(s) = \sum_{k=0}^{n} \frac{(n+k)!}{(n-k)!k!} (\frac{s}{2})^k$, and ω_0 is the cutoff frequency.

2. $$C_2(s) = \frac{a}{s + a}, \quad 0 < a < \infty. \tag{30}$$

3. $$C_3(s) = \frac{3a^2 s + a^3}{s^3 + 3as^2 + 3a^2 s + a^3}, \quad 0 < a < \infty. \tag{31}$$

4. $$C_4(s) = \frac{a_1}{s^n + a_n s^{n-1} + ... + a_1} \tag{32}$$

   where the parameters $a = (a_1, a_2, ..., a_n)$ are the solution of the following optimization problem:

   $$\min_{a \in \mathbb{R}^n} \|C_4(s)(1 - C_4(s))\|_{\mathcal{L}_1} \tag{33}$$

   subject to

   $$b_l \leq a_i \leq b_u \ \text{ and } \ C_4(s) \ \text{ stable} \tag{34}$$

   with $b_l \in \mathbb{R}$ and $b_u \in \mathbb{R}$ being the given lower and upper bounds respectively.

Remark 1 *$C_1(s)$ is the well known low-pass Bessel filter. $C_2(s)$ and $C_3(s)$ have been considered in Ref.[1] $C_4(s)$ is a filter obtained by constrained optimization method. We note that more general forms of $C_4(s)$ such as $\frac{b_m s^{n-1}+\ldots+b_1 s+a_1}{s^n+a_n s^{n-1}+\ldots+a_1}$ can also be considered. We use* `fmincon` *function in MATLAB optimization tool box to conduct the optimization procedure.*

Figure 3 displays the $\mathcal{L}_1$ gains of the above mentioned filters with respect to the bandwidth of each filter. Since we are concerned about the low frequency interval, the bandwidth is restricted to be less than $300 rad/s$. Note that we choose $C_4(s)$ as 3^{rd} order for convenience. It can be observed that $C_1(s)$ and $C_4(s)$ have the smallest $\mathcal{L}_1$ gain for $\|C(s)(1-C(s))\|_{\mathcal{L}_1}$. We also note that $\|C_2(s)(1-C_2(s))\|_{\mathcal{L}_1}$ is relatively small when the bandwidth is also small, but it increases dramatically as the bandwidth gets larger. We also observe the performance similarity of $C_1(s)$ (Bessel Filter) and $C_4(s)$. Figure 3 shows that $C_1(s)$ and $C_4(s)$ yield smaller $\mathcal{L}_1$-gains than the other two.

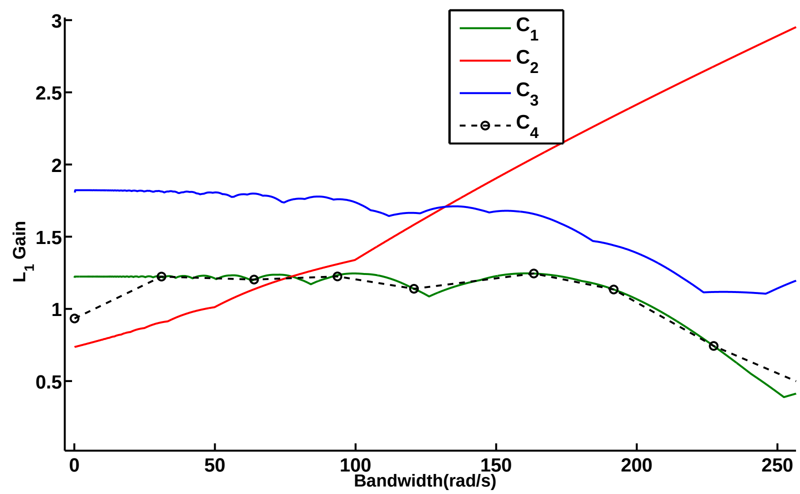

Figure 3. $\|C(s)(1-C(s))\|_{\mathcal{L}_1}, C(s) = C_i(s), i = 1, 2, 3, 4$

Figures 4(a) and 4(b) show the time-delay margins and the $\mathcal{L}_1$ gains for filters $C_1(s)$, $C_2(s)$ and $C_3(s)$ with respect to their bandwidths. Bessel filter $C_1(s)$ gives a larger time-delay margin compared to $C_2(s)$ and $C_3(s)$.

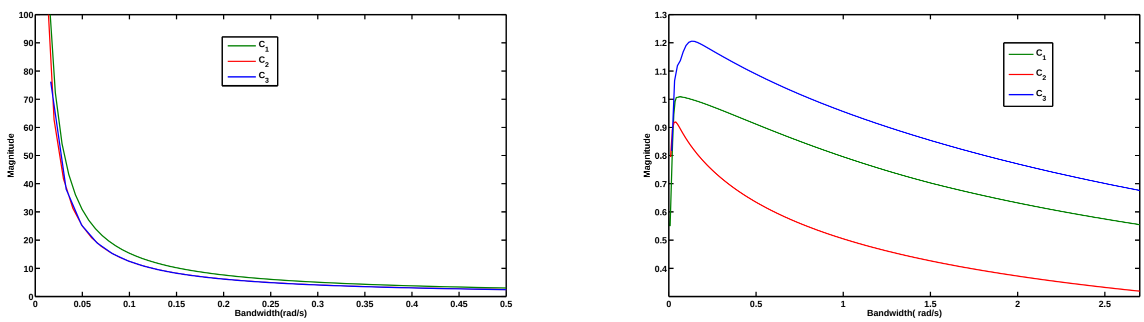

(a) Time-delay margins corresponding to $C_i(s), \quad i = 1, 2, 3.$

(b) $\mathcal{L}_1$ gains of $H(s)(1-C_i(s)), \quad i = 1, 2, 3.$

Figure 4. Time delay margins and $\mathcal{L}_1$ gains

VI. Filter Design Via Multi-Objective Optimization

In this section, the filter design procedure based on multi-objective optimization is given and is compared to the other three filters. By formulating a design objective, we can naturally present our design method as optimization of a single function representing the trade-off of two objectives (time-delay margin and $\mathcal{L}_1$-gain):

$$\min_a f(a) = \alpha\mathcal{T} + (1-\alpha)(-g), \quad 0 \le \alpha \le 1 \tag{35}$$

subject to stability of

$$C(s) = \frac{a_1}{s^n + a_n s^{n-1} + \dots + a_1}\,, \tag{36}$$

where $a = (a_1, a_2, \dots, a_n)^\top$, $\mathcal{T}$ is the time-delay margin of the open-loop transfer function $H_o(s)$, $g = \|H(s)(1 - C(s))\|_{\mathcal{L}_1}$, α is the weighting factor for the convex combination of $\mathcal{T}$ and g. Once an initial value a_0 and a factor α are given, the optimal filter $C(s)$ could be obtained by solving the above nonlinear constrained optimization problem.

We now take the 3^{rd} order filter as an example to show the feasibility of this multi-objective optimization method. Let $H(s) = \frac{1}{s+2}$, $\alpha = 0.9995$ and $a_0 = (1 \quad 3 \quad 3)^\top$. The following nonlinear, constrained optimization problem is solved by using the `fmincon` command of MATLAB optimization toolbox:

$$\min_{(a_1,a_2,a_3)} \alpha(-g) + (1-\alpha)\mathcal{T} \tag{37}$$

subject to

$$\begin{aligned} &-100000000 \le a_i \le 100000000, \quad i = 1, \dots, 3 \\ &\text{real part of each root of } s^3 + a_2 s^3 + a_1 s^2 + a_3 = 0 \le -0.2. \end{aligned} \tag{38}$$

The results are given in the first row of the following table The second row of the table has the $\mathcal{L}_1$ gain and the time-delay margin for a different third order filter $\frac{3\omega^2 s+\omega^3}{s^3+3\omega s^2+3\omega^2 s+\omega^3}$, $\omega = 0.795$ of the same bandwidth.

$C(s)$	$\mathcal{T}(sec.)$	$\|H(s)(1-C(s))\|_{\mathcal{L}_1}$	Bandwidth of $C(s)$ (rad/s)
$\frac{3.789e005}{s^3+3.521e004s^2+3.151e005s+3.789e005}$	1.4477	0.5126	1.3803
$\frac{19.97}{s^3+8.139s^2+22.08s+19.97}$	1.0087	0.8911	1.3804

The above result shows that a smaller $\mathcal{L}_1$ gain and larger time-delay margin can be obtained via appropriate optimization routines.

VI.A. The Impact of Weighting Factor α

Next we investigate the impact of the weighting factor α. Different values of α are chosen and tabled as follows:

α	$C(s)$	$\|C(s)(1-C(s))\|_{\mathcal{L}_1}$	g	$\mathcal{T}$ (*sec.*)	Bandwidth of $C(s)$ (*rad/s*)
0.005	$\frac{0.5624}{s^3+2.968s^2+3.689s+0.5624}$	0.8473	0.8997	7.3650	0.1747
0.05	$\frac{0.513}{s^3+4.006s^2+2.725s+0.513}$	0.9893	0.9103	5.3887	0.2555
0.5	$\frac{0.06681}{s^3+4.003s^2+3.393s+0.06681}$	0.4751	0.9103	62.5668	0.0201
0.95	$\frac{0.8166}{s^3+3.468s^2+3.082s+0.8166}$	1.0308	0.8803	3.7025	0.3764
0.995	$\frac{389600}{s^3+1693s^2+255600s+389600}$	0.7418	0.4262	2.3497	1.5362

From the table above, we could not determine an explicit relationship between α and $\mathcal{T}$ or the $\mathcal{L}_1$ gain. A significantly large $\mathcal{T}$ can be obtained if α is properly chosen ($\alpha = 0.5$ in this case). The $\mathcal{L}_1$ gain does not change much when α is adjusted.

VII. Conclusions

This paper addresses two different filter design methods for the $\mathcal{L}_1$ adaptive control architecture. Standard filter (Bessel filter) and optimization design methods have been considered to demonstrate the benefits of $\mathcal{L}_1$ adaptive controller from its design perspective. Its analytical performance bounds and time-delay margin can be used to the benefit of control engineers to achieve a desirable trade-off between performance and robustness.

VIII. Acknowledgments

The authors are thankful to Michael Steinhour from The Boeing Co. for useful comments and feedback.

References

[1] Cao, C. and Hovakimyan, N., "Design and Analysis of a Novel $\mathcal{L}_1$ Adaptive Control Architecture, Part I: Control Signal and Asymptotic Stability," *In Proc. of American Control Conference*, 2006, pp. 3397–3402.

[2] Cao, C. and Hovakimyan, N., "Design and Analysis of a Novel $\mathcal{L}_1$ Adaptive Control Architecture, Part II: Guaranteed Transient Performance," *In Proc. of American Control Conference*, 2006, pp. 3403–3408.

[3] Cao, C. and Hovakimyan, N., "Guaranteed Transient Performance with $\mathcal{L}_1$ Adaptive Controller for Systems with Unknown Time-varying Parameters: Part I," *American Control Conference*, 2007, pp. 3925–3930.

[4] Cao, C. and Hovakimyan, N., "Stability Margins of $\mathcal{L}_1$ Adaptive Controller: Part II," *American Control Conference*, 2007, pp. 3931–3936.

[5] Wise, K., Lavretsky, E., and et. al., "Adaptive Flight Control of a Sensor Guided Munition." *In Proc. of AIAA Guidance, Navigation and Control Conference*, 2005.

[6] Wise, K., Lavretsky, E., and Hovakimyan, N., "Adaptive Control in Flight: Theory, Application, and Open Problems." *In Proc. of American Control Conference*, 2006, pp. 5966–5971.

[7] Cao, C., Hovakimyan, N., and Lavretsky, E., "Application of $\mathcal{L}_1$ Adaptive Controller to Wing Rock," *In Proc. of AIAA Guidance, Navigation and Control Conference*, 2006.

[8] Wang, J., Cao, C., Patel, V., Hovakimyan, N., and Lavretsky, E., "$\mathcal{L}_1$ adaptive neural network controller for autonomous aerial refueling with guaranteed transient performance," *In Proc. of AIAA Guidance, Navigation and Control Conference*, 2006.

[9] Beard, R. W., Knoebel, N., Cao, C., Hovakimyan, N., and Matthews, J., "An $\mathcal{L}_1$ Adaptive Pitch Controller for Miniature Air Vehicles," *In Proc. of AIAA Guidance, Navigation and Control Conference*, 2006.

[10] Pomet, J. and Praly, L., "Adaptive nonlinear regulation: Estimation from the Lyapunov equation," *IEEE Trans. Autom. Contr.*, Vol. 37(6), June 1992, pp. 729–740.